

Self-organization of polymer nanoneedles into large-area ordered flowerlike arrays

Dong Wu,¹ Qi-Dai Chen,¹ Bin-Bin Xu,¹ Jian Jiao,¹ Ying Xu,¹ Hong Xia,¹ and Hong-Bo Sun^{1,2,a)}

¹State Key Laboratory on Integrated Optoelectronics, College of Electronic Science and Engineering, Jilin University, 2699 Qianjin Street, Changchun 130012, People's Republic of China

²College of Physics, Jilin University, 119 Jiefang Road, Changchun 130023, People's Republic of China

(Received 18 April 2009; accepted 8 August 2009; published online 31 August 2009)

Combination of top-down and bottom-up process is crucial for fabricating ordered complex micronanostructures. Here we report a simple, rapid, and versatile approach to demonstrate this useful concept, which involves the joint use of multibeam interference patterning and capillary force self-organization. Regular hydrophobic arrays of four-peddle nanoflowers consisting of bent needles with 300 nm tip diameters are readily produced. A “domino model” based on the balance of the capillary and support forces were proposed to interpret realization of large-area homogeneity of the array. The technology, promising for preparing more complex and functional structures, may find broad utilization in nano and biological researches. © 2009 American Institute of Physics.

[DOI: 10.1063/1.3213394]

Preparation of ordered complex micronanoarchitectures in a controlled fashion is of great importance to nanoscience and technology, which is driving the progress of microfabrication techniques based on electron-beam, ion-beam, UV, electron beam lithography, and two-photon induced photopolymerization.¹ Despite the fact that well-controlled structures such as gratings, pillar arrays,^{2,3} and photonic crystals⁴ have been accomplished by the top-down methods, achievable geometry is limited to relatively simple ones, particularly to those with planar layout. In contrast, self-assembly is a convenient bottom-up approach that can make complex three-dimensional (3D) architecture⁵ such as trees, flowers, and photonic structures⁶ by natural forces. It, however, is weak in the controllability of the pattern formation. By combining the top-down microfabrication and the bottom-up self-assembly, regular complex structures made of ordered ZnO nanorods,⁷ spherical colloids,⁸ copolymer blocks,⁹ and functional sol-gel materials^{10,11} were realized. Among these works, polymers, due to their better biocompatibility, are attracting particular attentions for application as their biomimic structured surfaces.¹² However, realization of the surface micronanostructures is restricted to particular material species, and it is difficult to produce secondary patterns on ready structures because of the use of molds for pattern replica.^{8–12} This problem can be solved by multibeam interference, a technology featuring elimination of molds, less restraint to substrate, abundance of achievable patterns, and diversity of useful materials, for the top-down fabrication of the precursory micronanopatterns. As the first step toward this direction, we reported in this letter the production of large-area uniform periodic nanoflowers arrays by interference patterning aided with capillary force self-organization. In the interference step, polymer needles are created as the fundamental building blocks, and then they are attracted together by capillary force, four in a group, to form regularly arrayed flowerlike patterns.

Figure 1(a) schematically shows the fabrication process of period nanoflower arrays. It consists of the following four steps: spin coating, multibeam interference, developing, and drying. First, a glass slide was cleaned with acetone and absolute ethanol, and then the photoresist (Norland, NOA 61) was spin coated at 500 rpm for 18 s, by which a 3 μm thick film was formed. Second, a frequency-tripled, *Q*-switched, single-mode neodymium dope yttrium aluminum garnet nanosecond laser with 355 nm wavelength and 10 ns pulse width (Spectra-physics) was utilized as the irradiance light source. The output laser light was split into four beams, all with ~ 10 mm diameter and 80 mW power. They were overlapped on the sample both temporally and spatially by adjusting the optical path length rigorously. A periodic light intensity pattern was formed by the interference of the beams. It was then fixed by the negative photoresist through photopolymerization, whereby regions of high light intensity

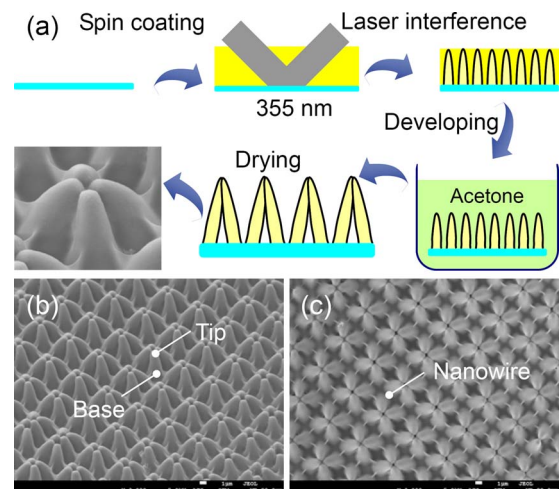


FIG. 1. (Color online) Fabrication of regular flowerlike arrays by combinative use of multibeam interference patterning and capillary force self-organization. (a) The fabrication process: spin coating, laser beam interference, development, and drying. (b) and (c) are 45°-tilted and bird's eye view SEM images of the array.

^{a)}Author to whom correspondence should be addressed. Electronic mail: hbsun@jlu.edu.cn. Homepage: <http://www.lasun-jlu.cn/>

are cross linked and are solidified. The exposure duration, easily adjusted by an optical shutter, is here 6 s. In the third step, unreacted or less-polymerized monomers or oligomers were dissolved by acetone solvent and a solidified squarely periodic needle arrays structure was left. The periodicity of the structure, d , is determined by the interference angle, θ_{air} (the angle between the main optical axis and the incident beams in air), and the wavelength λ according to $d = \lambda / (\sqrt{2} \sin \theta_r)$. Given $\theta = 5.8^\circ$, we have $d = 2.5 \mu\text{m}$. In the fourth step, uniform nanoflowers arrays were obtained when the acetone solvent was evaporated [Fig. 1(b)]. Judging from the top view scanning electron microscopic (SEM) image, individual flower consists of four petals, each bent from a needle produced from the interference patterning. It is easy to find that in Fig. 1(c) the height of the needle is around $3 \mu\text{m}$, as is equal to the thickness of the resin layer and is freely adjustable according to structure design. The tip radius of the needle is as small as 300 nm , which is sensitively dependent on the developing condition.²

The prerequisite for the nanoflower formation is the needle bending, which is considered as a result of capillary forces occurring in the liquid/vapor menisci between nearest neighboring polymer needles.¹³ Whether a needle is kept standing upright or bent aside is determined by the relative magnitude of the supporting force F_s (Ref. 12) and the capillary force,¹⁴

$$F_{\text{att}} = 2\pi S \gamma \cos \alpha / \delta, \quad (1)$$

where S is the area of the side plane of a cuboid rod in the model adopted for the simplicity of analysis [Fig. 3(a)], γ , α , and δ are the surface tension, the contact angle, and the space between the two planes. $F_s \sim Er^4d/h^3$ is defined as the critical force that causes the needle bending, where E , r , d , and h are the Young's modulus, the distance, and the height of the needles, respectively. It is proportional to the fourth order of their diameter, interneedle distance and the inverse of the third order of the needle height.¹² It is seen that large needle diameter, large interneedle distance, or small needle height aids a needle to stand unbent, according to both of the formulas of the supporting force F_s and the capillary force F_c . If the solvents are homogeneously removed ($F_{\text{att}} = 0$), or even if any nonuniformity of forces exists but $F_{\text{att}} < F_s$, the rods would stay erect. It is interesting to notice there are nanowires with sub-100 nm diameter formed between the adjacent needles. According to our previous study,² these nanowires were produced as remnant of the menisci interface between the air and solvent by carefully controlling the developing duration. Here, we find the wire diameter and the number is also sensitively affected by the exposure dose. Experimentally, we tuned the exposure duration from 3, 4, 5, and 8 s, while the laser power remained identical. There are no nanowires for short exposure duration 3 s [Fig. 2(a)]. When it is increased to 4 s, the nanowire begins to appear, but very thin [Fig. 2(b)]. 5 s exposure produces much wider connecting wires [Figs. 2(c) and 2(d)]. When the exposure duration is extended to 8 s, needles become robust enough to counteract the capillary force so that no flowerlike array is formed. Similarly, nanowire is generated when the needle height is reduced, for example, $h = 1.5 \mu\text{m}$ [Figs. 2(e) and 2(f)].

Another important question that needs answering is how such a high regularity in the formation of the four-pedal

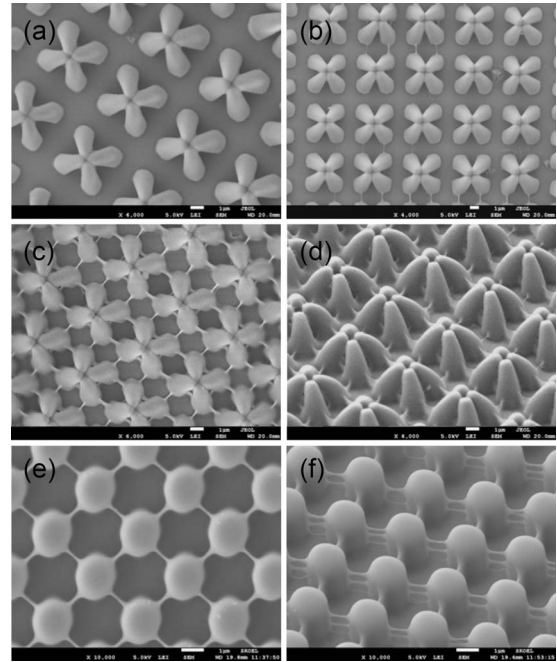


FIG. 2. Complex periodic nanostructures under varied exposure conditions. (a)–(c) are top-view SEM images of nanoflowers formed under exposure of 3, 4, and 5 s, respectively. (d) 45°-tilted SEM image of the 5 s exposed nanoflower array. (e) and (f) are top and tilted view SEM images of complex network arrays produced from $1.5 \mu\text{m}$ thick sample by long exposure of 8 s.

flowerlike structures has been attained, and whether it is possible to further increase the area of uniform arrays to the current hundreds of square micrometers. A model was proposed based on the assumption that the freestanding needles are unstable due to the strong capillary attraction [Figs. 3(a) and 3(b)]. With an external stimuli like dragging of liquid/air

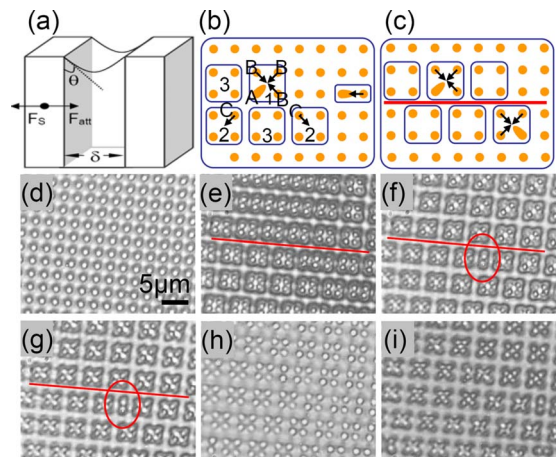


FIG. 3. (Color online) Domino model for interpreting the formation of nanoflowers. (a) A cuboid rod pair for illustrating the forces interacting on a rod. Between the two cuboids is the liquid solvents with the curved surface. (b) Illustrative Domino effect on the four-peddle group (flower) formation, where starting from the triggering center A, groups 1, 2, and 3 are sequentially produced. (c) Generation of more than one domains as a result of the creation multiple triggering center. (d) The needle arrays stand itself in acetone solvent. (e) Four needles are bonded together with the evaporation of the solvent, notice the special case of grouped six needles in the framed region. (f) One pair of needles is separated, producing a two-peddle flower. (g) Evaporation is completed. (h) The needles are released from the flower when the structure was immersed in the solvent, and (i) recovered to the original flower status when the solvent is evaporated once more.

interface, air blowing, or solvent floating, some a rod, for example, rod A may lean, as raises the attraction between A and its nearest rods B's because F_{att} is inversely proportional to the inter-rod distance [Eq. (1)]. As a result, three rods B's are attracted to A, producing nanoflower one. For the same reason, the reduction of the capillary between A and C's due to the increased inter-rod distance (δ_{ac}) leads to titling of rods C's to the direction opposite to rod A and the formation of nanoflower group 2. The chain tilting of needles is thus triggered and propagated from A to its surrounding by the *Domino effect*, and groups 1, 2, and 3 are sequentially produced. As a quite rare case, if the bending direction of a triggering rod is exactly parallel to a line of nearest rods, there will be only one rod that is attracted by it. As result, a two-peddle group may be formed [Fig. 3(b)]. Such a phenomenon did be observed, as shown by the circled region in Figs. 3(f) and 3(g). The rods bending and connection were observed occurring in time range of milliseconds, too fast to be captured by a general video camera, 25–30 frame/s. However, if the above model is true, more domains may take shape if it happens that more than one “trigger centers” are produced [Fig. 3(c)]. Such a multiple domain structures are also observed as shown in Figs. 3(e)–3(g). The upper and the lower parts of the arrays grow apparently from two different centers so that they are offset by half a period. The important roles played by the relative magnitude of the capillary and supporting forces is thus approved, and could be further manifested by immersing the flowerlike structure back into the solvent, meaning that the capillary force was withdrawn. The needles basically recovered to upstraight position [Fig. 3(h)]. The residual curvature (notice that the rods do not stand completely erect as they were initially created [Fig. 3(d)]) helps them to remember their previously formed shapes when the solvent is removed once more [Fig. 3(i)].

According to the above model, the trigger centers may be purposely induced with a reduced number by tilting the substrate, as leads to a thinner film of the solvent at the lifted end. Once a single trigger center, as well as a nanoflower group is created, its propagation to the lower side will be accelerated following the movement of the evaporation front from the upper to lower side. This equivalently reduces formation probability of other triggering centers, helping the preparation of large area uniform samples. Experimentally, the above idea is tested and proved: a 30° tilt angle gives rise to a single-domain area of more than 60 mm^2 , which was decided by the size of four laser beams ($\sim 9 \text{ mm}$). Shown in Figs. 4(a) and 4(b) are two single-domain area of more than $1000 \mu\text{m}^2$ under different laser dosage. It is not surprising such a large area array exhibits good hydrophobic ability

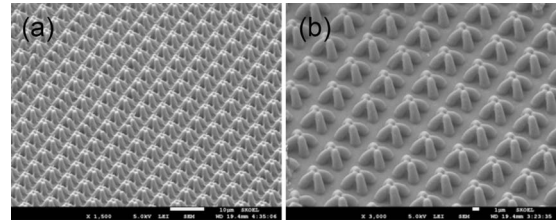


FIG. 4. The uniform, controllable, and large-area nanoflower arrays realized by the sample-tilted method. (a) and (b) are two types of uniform nanoflowers arrays under exposure times of 5 and 3 s.

because the needle morphology reduces the effective contact area with the water droplet.^{15–17}

In summary, we have fabricated complex nanoflower arrays by a combination of the top-down laser micronanofabrication and the bottom-up self-organization. The balance of the capillary and supporting forces, as summarized as a Domino effect model, was found playing an important role in the formation of the large-area highly regular four-peddle flower arrays. The simplicity, designability, and reproducibility of approach would permit realization of more complicated and functional structures for broad applications of the micronanostructures in nano and biological researches.

The authors thank NSFC for support under Grant Nos. 60525412 and 60677016.

¹D. Wu, L. G. Niu, Q. D. Chen, R. Wang, and H. B. Sun, *Opt. Lett.* **33**, 2913 (2008).

²H. B. Sun, A. Nakamura, S. Shoji, X. M. Duan, and S. Kawata, *Adv. Mater.* **15**, 2011 (2003).

³H. B. Sun, A. Nakamura, K. Kaneko, S. Shoji, and S. Kawata, *Opt. Lett.* **30**, 881 (2005).

⁴D. Xu, K. P. Chen, K. Ohlinger, and Y. Lin, *Appl. Phys. Lett.* **93**, 031101 (2008).

⁵Z. R. Tian, J. Liu, J. A. Voigt, B. Mchenzie, and H. Xu, *Angew. Chem., Int. Ed.* **42**, 413 (2003).

⁶X. Gao, X. Li, and W. Yu, *J. Phys. Chem. B* **109**, 1155 (2005).

⁷J. W. P. Hsu, Z. R. Tian, N. C. Simmons, C. M. Matzke, J. A. Voigt, and J. Liu, *Nano Lett.* **5**, 83 (2005).

⁸Y. Xia, Y. Yin, Y. Lu, and J. McLellan, *Adv. Funct. Mater.* **13**, 907 (2003).

⁹J. Cheng, A. M. Mayes, and C. A. Ross, *Nature Mater.* **3**, 823 (2004).

¹⁰A. Sidorenko, T. Krupenkin, A. Taylor, P. Fratzl, and J. Aizenberg, *Science* **315**, 487 (2007).

¹¹D. Chandra, J. A. Taylor, and S. Yang, *Soft Matter* **4**, 979 (2008).

¹²B. Pokroy, S. H. Kang, L. Mahadevan, and J. Aizenberg, *Science* **323**, 237 (2009).

¹³T. Eisner and D. J. Aneshansley, *Proc. Natl. Acad. Sci. U.S.A.* **97**, 6568 (2000).

¹⁴J. N. Israelachvili, *Intermolecular and Surface Forces*, 2nd ed. (Academic, London, 1992).

¹⁵W. L. Min, B. Jiang, and P. Jiang, *Adv. Mater.* **20**, 3914 (2008).

¹⁶L. Zhai, F. C. Cebeci, R. E. Cohen, and M. F. Rubner, *Nano Lett.* **4**, 1349 (2004).

¹⁷A. B. D. Cassie and S. Baxter, *Trans. Faraday Soc.* **40**, 546 (1944).